SCANNING VOL. 23, 328–336 (2001)

Received: February 6, 2001
Accepted: May 16, 2001

Single-Image Signal-to-Noise Ratio Estimation

J. T. L. THONG, K. S. SIM, J. C. H. PHANG

Centre for Integrated Circuit Failure Analysis and Reliability (CICFAR), Faculty of Engineering, National University of Singapore, Singapore

Summary: A method for estimating the signal-to-noise ratio from a single image is presented in this paper. The autocorrelation-based technique requires that image details be correlated over distances of a few pixels, while the noise is assumed to be uncorrelated from pixel to pixel. The latter is shown to be a good approximation in the case of scanning electron microscope (SEM) images provided that the video signal is not band limited. The noise component is derived from the difference between the image autocorrelation at zero offset and an estimate of the corresponding noise-free autocorrelation. Nonlinear effects introduced by intensity saturation and their implications on the image signal-to-noise ratio are also discussed.

Key words: scanning electron microscopy, image signal-to-noise ratio, noise, autocorrelation

PACS: 07.78.+s, 05.40.Ca, 07.05.Pj

Introduction

Quantification of the signal-to-noise ratio (SNR) is important in image acquisition procedures in electron microscopy and other fields where the image is degraded by noise. In particular, with scanning electron microscopy (SEM), the tradeoff with image resolution is often SNR. The definition of SNR varies according to the field. In electrical engineering and statistical optics, it is defined as the energy (variance) ratio between signal and noise, while in the electron microscopy literature the square root of this quantity is usually considered.

The cross-correlation technique could be used to estimate the SNR of band-limited stochastic functions. Frank and Al-Ali (1975) formulated the use of cross correlation to derive the SNR from two microscope images of the same specimen area. The method distinguishes between image detail and random noise, since true image information detail is present in both copies of the micrograph whereas random noise, although present in both cases, is not correlated from pixel to pixel. Erasmus (1982) used the same method for measuring the improvement in SNR with digital image averaging. More recently, Joy *et al.* (2000) used the cross-correlation function to evaluate the resolution and SNR performance of critical dimension (CD)-SEMs. In another field, Sijbers *et al.* (1996) based their SNR evaluation of magnetic resonance imaging (MRI) images on the seminal work of Frank and Al-Ali. However, the primary disadvantage of using two-image SNR determination methods is the requirement that the two images be perfectly aligned. Moreover, it cannot be used to determine the SNR of an extant image such as a stored image or micrograph.

This paper presents a method that uses one image instead of two for estimating the SNR. Since only a single image is required, the proposed method is not constrained by image registration requirements, and it can be applied in real time in cases where image drift is present in the SEM. In a modern personal computer (PC) SEM, adaptive control of the number of averages to attain a desired SNR can be envisaged using this technique.

Calculating Signal-to-Noise Ratio from Two Images

Frank (1980) developed the two-image SNR theory based on the cross correlation of two image acquisitions of the same object. The cross-correlation coefficient of the two images can be defined as

$$\rho_{12} = \frac{\phi_{12}(0) - \mu_1\mu_2}{\sigma_1\sigma_2} \tag{1}$$

where $\phi_{12}(0)$ is the peak height of the cross-correlation function (CCF) of the two images in aligned position, and μ_1,μ_2 and σ_1,σ_2 are the means and variance values of the two images, respectively. The SNR is then

$$SNR = \frac{\rho_{12}}{1-\rho_{12}} \tag{2}$$

Address for reprints:

John T. L. Thong
Department of Electrical and Computer Engineering
National University of Singapore
4 Engineering Drive 3
Singapore 117576
E-mail: elettl@nus.edu.sg

where it is assumed that the two image acquisitions contain the same signal, but with uncorrelated noise of zero mean. The procedure for estimating the SNR thus involves choosing two images from the experimental image set, aligning them, and evaluating Eq. (2). To reduce the variance in the SNR estimate, an average of estimates can be obtained from several randomly selected image pairs (Frank 1996).

Single-Image Estimate of Signal-to-Noise Ratio

The proposed method for deriving the SNR from one image starts from Eq. (1) for two images of identical signal but uncorrelated noise, viz.

$$\rho_{12} = \frac{\phi_{12}(0) - \mu_1\mu_2}{\sigma_1\sigma_2}$$

$\phi_{12}(0)$ is the CCF between images $f_1(x,y) = s_1(x,y) + n_1(x,y)$ and $f_2(x,y) = s_2(x,y) + n_2(x,y)$ at zero offset, where s_1 and s_2 represent the noise-free images, and n_1 and n_2 are the noise content of these two images. Since we are dealing with images, the CCF, $\phi_{12}(x,y)$, is two-dimensional. For simplicity, in the following we will normally illustrate the correlation function with offset along the x direction at zero y offset.

Since (1) n_1 and n_2 are uncorrelated, and (2) the noise is assumed to be uncorrelated with the signal, then

$$\begin{aligned}\phi_{12}(0,0) &= \frac{1}{N^2}\sum_{j=0}^{N-1}\sum_{i=0}^{N-1}\big(s_1(i,j)+n_1(i,j)\big)\big(s_2(i,j)+n_2(i,j)\big)\\ &\cong \frac{1}{N^2}\sum_{j=0}^{N-1}\sum_{i=0}^{N-1}s_1(i,j)\cdot s_2(i,j) = \phi_{12}^{NF}(0,0)\end{aligned} \tag{3}$$

where $\phi_{12}^{NF}(0,0)$ denotes the CCF between the two noise-free images, s_1 and s_2, at zero offset. Furthermore, since the noise-free images are identical, we have $s_1 = s_2$ and thus

$$\phi_{12}(0,0) = \phi_{12}^{NF}(0,0) = \phi_{11}^{NF}(0,0) \tag{4}$$

where $\phi_{11}^{NF}(0,0)$ is the value of the autocorrelation function (ACF) of the noise-free image at zero offset.

Since the two images have identical signal corrupted with noise of zero mean, the mean values of both images are identical. Thus

$$\mu_1 = \mu_2 \tag{5}$$

The variance of image 1, σ_1, is given by

$$\sigma_1^2 = \frac{1}{N^2}\sum_{j=0}^{N-1}\sum_{i=0}^{N-1}\big(f_1(i,j)-\mu_1\big)^2 = \phi_{11}(0,0) - \mu_1^2$$

Similarly for image 2,

$$\sigma_2^2 = \phi_{22}(0,0) - \mu_2^2$$

Since $\phi_{11}(0,0) = \phi_{22}(0,0)$, we obtain

$$\sigma_1^2 = \sigma_2^2 = \sigma_1 = \sigma_2 \tag{6}$$

From Eqs. (4)–(6),

$$\rho_{12} = \rho_{11}^{NF} = \frac{\phi_{11}^{NF}(0,0) - \mu_1^2}{\sigma_1^2}$$

$$\therefore SNR = \frac{\rho_{12}}{1-\rho_{12}} = \frac{\phi_{11}^{NF}(0,0)-\mu_1^2}{\sigma_1^2 - \phi_{11}^{NF}(0,0) + \mu_1^2} = \frac{\phi_{11}^{NF}(0,0)-\mu_1^2}{\phi_{11}(0,0) - \phi_{11}^{NF}(0,0)} \tag{7}$$

Thus, the SNR of a single image can be obtained from the ACF curve (Fig. 1). As shown in the figure, $\phi_{11}(0,0) - \phi_{11}^{NF}(0,0)$ represents the noise energy and $\phi_{11}^{NF}(0,0) - \mu_1^2$ represents the signal energy, where μ_1 is the mean value of image,

$$\mu_1 = \frac{1}{N^2}\sum_{j=0}^{N-1}\sum_{i=0}^{N-1} f_1(i,j)$$

Unfortunately, with a single image corrupted by noise, $(s_1 + n_1)$, $\phi_{11}^{NF}(0,0)$ cannot be obtained directly since the noise n_1 is correlated at zero offset and

$$\begin{aligned}\phi_{11}(0,0) &= \frac{1}{N^2}\sum_{j=0}^{N-1}\sum_{i=0}^{N-1}\big(s_1(i,j)+n_1(i,j)\big)\big(s_1(i,j)+n_1(i,j)\big)\\ &= \frac{1}{N^2}\sum_{j=0}^{N-1}\sum_{i=0}^{N-1}s_1^2(i,j)+n_1^2(i,j)\\ &\neq \phi_{11}^{NF}(0,0)\end{aligned}$$

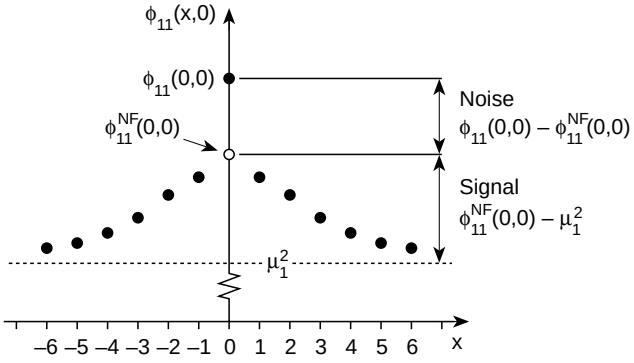

FIG. 1 Representation of signal and noise components on a plot of the autocorrelation function. The filled markers represent the data derived from the image.

Since $\phi_{11}^{NF}(0,0)$ is unknown, a method for estimating $\phi_{11}^{NF}(0,0)$ is required.

Estimation of Noise-Free Autocorrelation

To estimate $\phi_{11}^{NF}(0,0)$, we need to separate the signal from the noise based solely on the information available in the single image. On a pixel-by-pixel basis, it is impossible to distinguish the signal from the noise unless some a priori assumptions are made about the nature of the signal and noise.

First, consider the noise. A primary assumption of the proposed technique is that the noise is uncorrelated from pixel to pixel. For noise that is white and stationary, its power spectrum (optical transfer function) is uniform. Since the power spectrum and the ACF are a Fourier transform pair, then the ACF of such noise is a delta function at zero offset (Fig. 2a). On the other hand, if the noise is non-white, then the ACF will have finite values at offsets other than zero (Figure 2b). For SEM secondary emission signals limited by shot-noise in the beam, the power spectrum of the noise is generally white, provided that the video signal is not band-limited (although cold-field emission sources with significant flicker noise will give rise to a pinkish content). This is easily demonstrated by analyzing the ACF of the image acquired from a featureless specimen. Figure 3 shows the image of a bare silicon wafer and the corresponding ACF at small offsets calculated in the *x* and *y* directions. The ACF in the *x* direction shows a transition over two pixels, whereas the ACF in the *y* direction is indeed a delta function at the origin. The disparity arises from the finite impulse response time of the SEM video chain, which shows up as image smearing in the direction of the raster scan (*x* direction), but not in the *y* direction since an entire line period has lapsed between two adjacent pixels in the direction of the frame scan. At slower scan rates, the ACF in the *x* direction would tend toward a delta function.

For the signal part, specimen details that are imaged as single pixels cannot be distinguished from noise. Hence, for example, if we have a single image of a highly detailed specimen taken at low magnification, such that the image

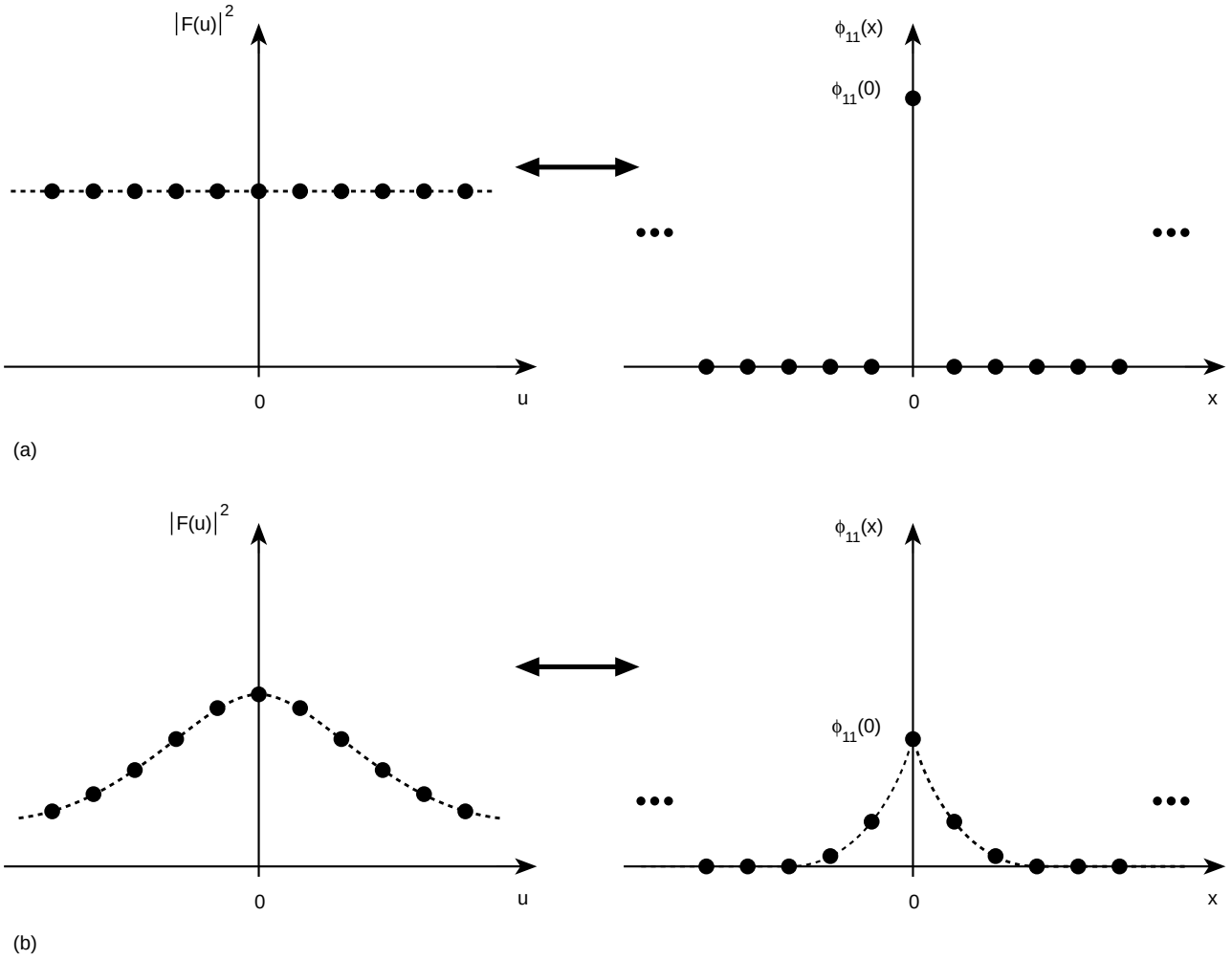

FIG. 2 Fourier transform pairs for (a) white noise and (b) band-limited noise.

contrast varies greatly from pixel to pixel, then one is unable to determine the extent to which the image is corrupted by noise (Fig. 4). On the other hand, SEM images taken at magnifications sufficient to define the features of the specimen will have details covering at least several image pixels. In other words, such details correlate over distances of a few pixels. This then provides a means to estimate $\phi_{11}^{NF}(0,0)$ from the ACF at small offsets from the origin. The noise component, which is confined to the origin of the ACF, is then $\phi_{11}(0,0) - \langle\phi_{11}^{NF}(0,0)\rangle$

The simplest estimate of $\phi_{11}^{NF}(0,0)$ is to assume that it is the same as the ACF at neighboring offsets (Fig. 5a), that is,

$$\left\langle \phi_{11}^{NF}(0,0) \right\rangle \approx \phi_{11}(1,0) = \phi_{11}(-1,0) \tag{8a}$$

Returning to two dimensions (Fig. 5b), if we consider unit offset in the x and y directions of ACF, the values can be averaged,

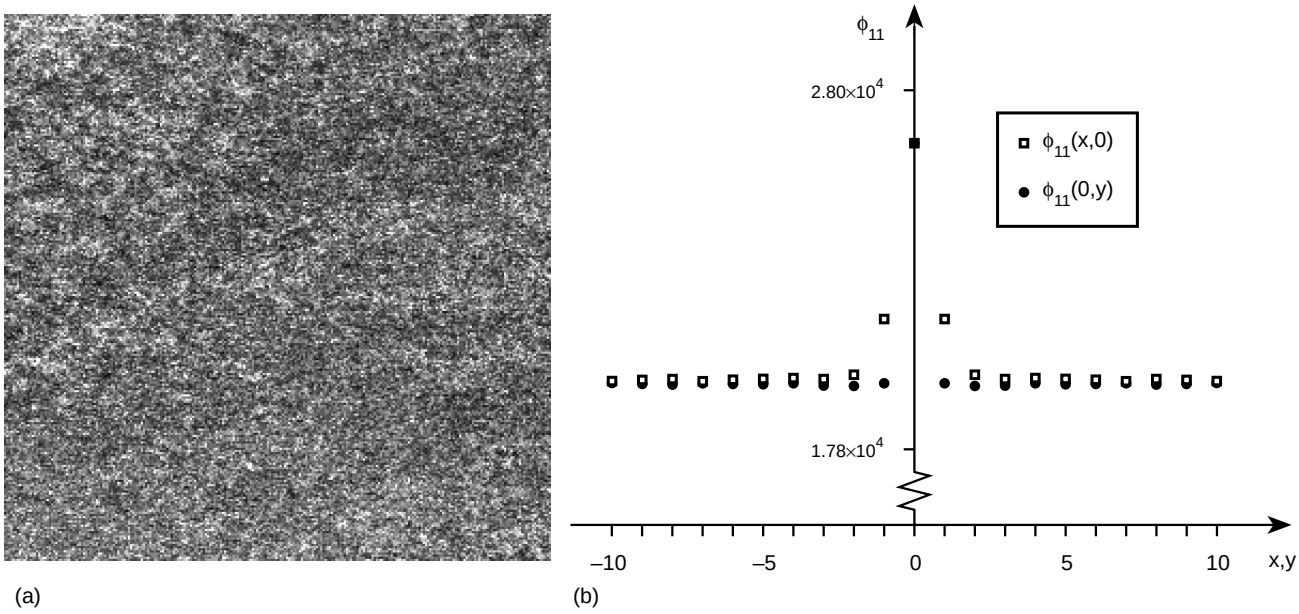

FIG. 3 (a) Noisy SEM image of bare silicon wafer (256×256 pixels). The raster line scan is in the x direction. (b) Autocorrelation function at small offsets along the x direction (y = 0) and the y direction (x = 0).

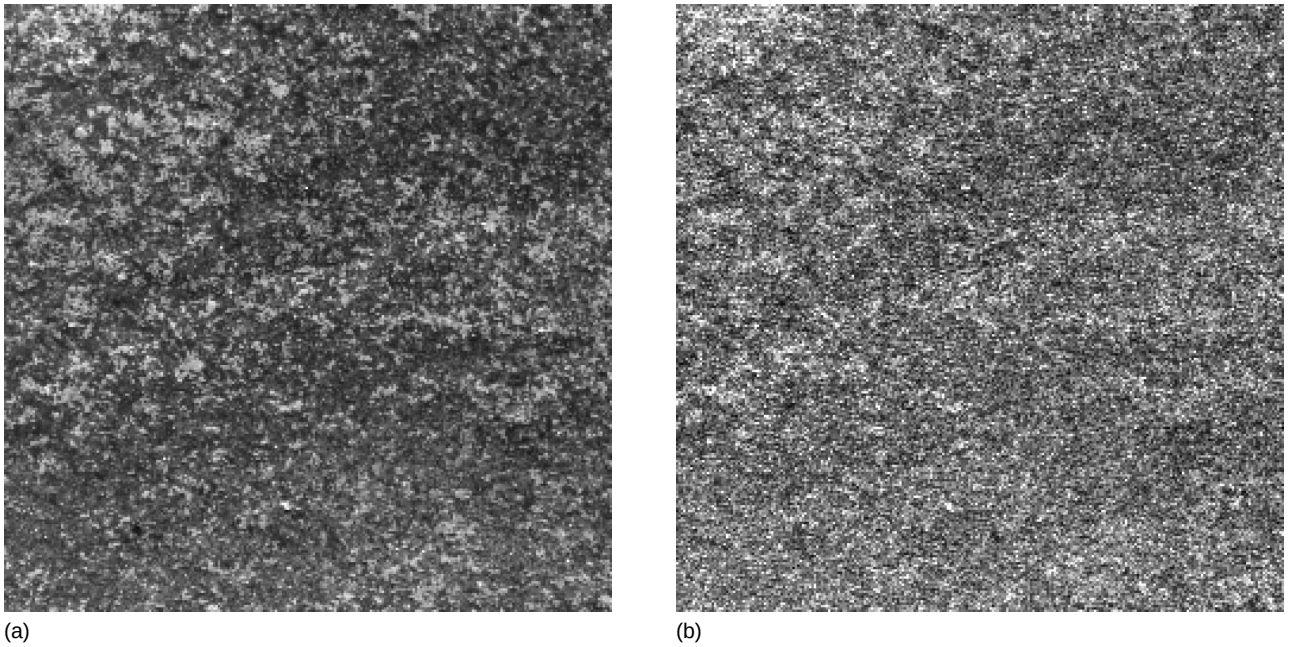

FIG. 4 (a) Noise-free and (b) noisy image of the same area of silver paint taken at low magnification. Image size = 256×256 pixels. Horizontal field width = 500 μm.

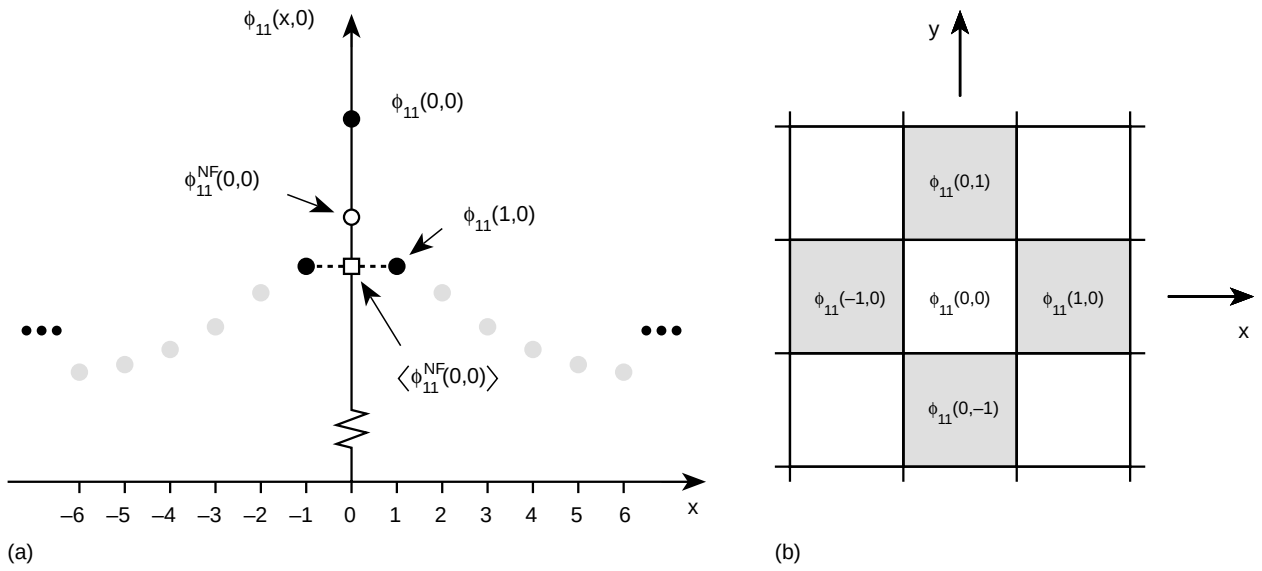

FIG. 5 Estimation of $\phi_{11}^{NF}(0,0)$ by assigning the autocorrelation function values at neighboring offsets (a) along the *x*-direction, (b) along both *x* and *y* directions.

$$\left\langle \phi_{11}^{NF}(0,0)\right\rangle \approx \frac{\phi_{11}(1,0)+\phi_{11}(0,1)}{2} \tag{8b}$$

This estimate would be reasonable if the ACF of the noise-free image changes slowly around the origin, which would be true for images where the details correlate over many pixels.

A better approach might be to apply a first-order extrapolation. If we consider the *x* direction, as shown in Figure 6, the adjacent points $\phi_{11}(1,0)$ and $\phi_{11}(2,0)$ can be used to project $\phi_{11}^{NF}(0,0)$ and would in most cases be an improvement on the estimate of Eq. (8a). Higher-order functions, such as polynomials, can be used to fit the ACF curve, but whether the results returned by such fitting functions would provide a closer estimate will depend on the nature of the image.

To illustrate the above methods for estimating $\phi_{11}^{NF}(0,0)$, heavily averaged images of silver paint that are practically free of noise are first taken at magnifications (as indicated on the SEM) of 5k× and 1k×. White noise is then added to the images, as shown in Figure 7a and b, respectively, resulting in the corresponding ACFs shown at small offsets in the *x* direction. Artificial addition of noise is carried out instead of capturing a second noisy image to avoid the uncertainties associated with comparing two images. The actual values of $\phi_{11}^{NF}(0,0)$ are derived from the original noise-free image. In both cases, the simple approximation of Eq. 8(a) invariably underestimates $\phi_{11}^{NF}(0,0)$, while the first-order extrapolation method underestimates in one case and overestimates in the other. For these examples, the latter method provides better estimates (Table I).

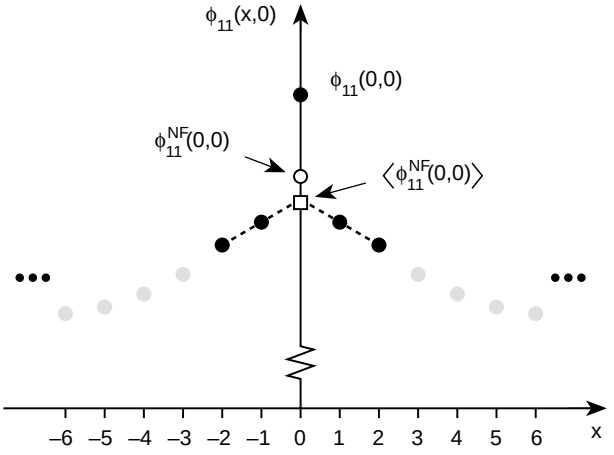

FIG. 6 Estimation of $\phi_{11}^{NF}(0,0)$ by a first-order extrapolation from neighboring offsets along the *x*-direction.

Implementation

The discrete cross correlation between two images of size N^2, $f_1(x,y)$ and $f_2(x,y)$, is given by

$$\phi_{12}(x,y)=\frac{1}{N^2}\sum_{j=0}^{N-1}\sum_{i=0}^{N-1} f_1(i+x,j+y)\cdot f_2(i,j)=\phi_{21}(-x,-y)$$

It follows that the autocorrelation of image $f_1(x,y)$ is then

$$\phi_{11}(x,y)=\frac{1}{N^2}\sum_{j=0}^{N-1}\sum_{i=0}^{N-1} f_1(i+x,j+y)\cdot f_1(i,j)=\phi_{11}(-x,-y) \tag{9}$$

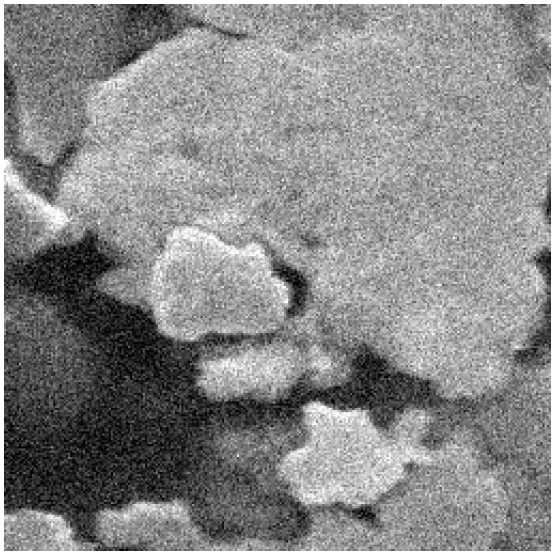

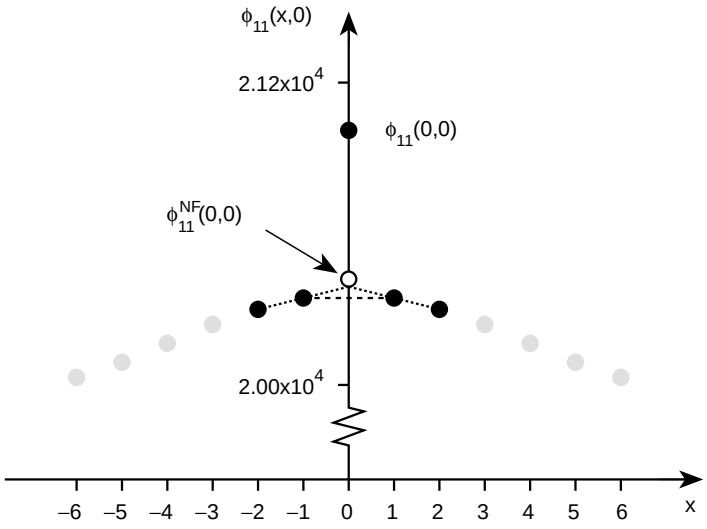

(a)

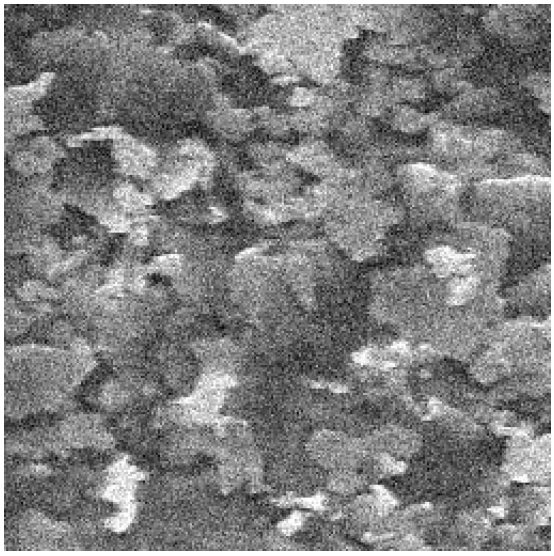

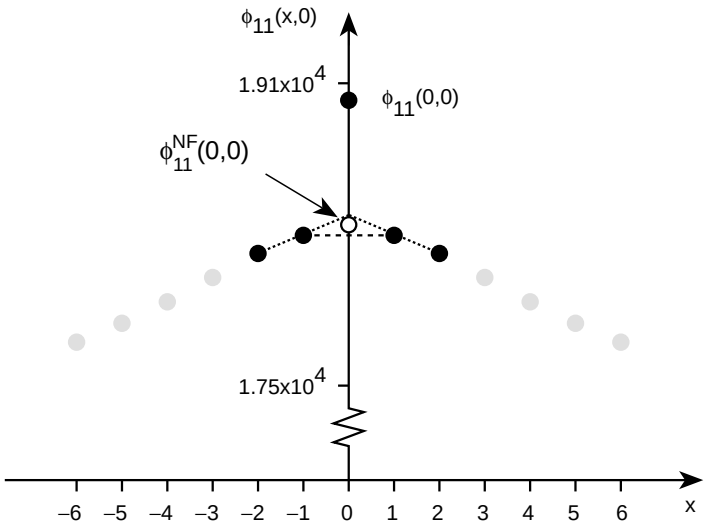

(b)

FIG. 7 Images of silver paint with added noise at (a) higher magnification (horizontal field width = 5 μm), and (b) lower magnification (horizontal field width = 25 μm), and corresponding autocorrelation function (ACF) along the *x*-direction, showing the two techniques to estimate the noise-free image autocorrelation. Unfilled marker indicates the actual value of the ACF for the noise-free image. Images are 256×256 pixels.

TABLE I Parameters derived from the noisy images. The actual value of $\phi_{11}^{NF}(0,0)$ is obtained from the original noise-free images before noise was added in artificially

	μ_1^2	$\phi_{11}(0,0)$	$\phi_{11}^{NF}(0,0)$ Actual value	$\langle\phi_{11}^{NF}(0,0)\rangle = \phi_{11}(1,0)$	$\langle\phi_{11}^{NF}(0,0)\rangle$ 1st order extrapolation
5k× image	18045	21015	20421 (SNR = 4.00)	20345 (SNR = 3.43)	20387 (SNR = 3.73)
1k× image	17061	18992	18367 (SNR = 2.09)	18312 (SNR = 1.84)	18408 (SNR = 2.31)

Abbreviation: SNR=signal-to-noise ratio.

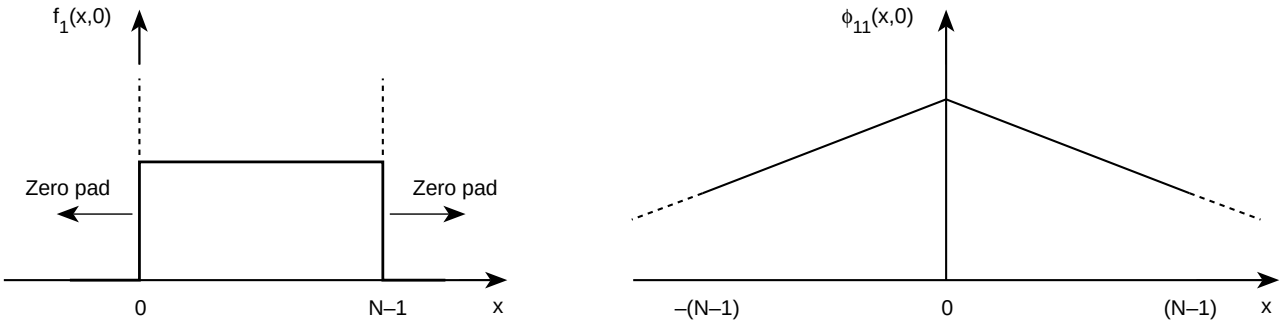

FIG. 8 Effect of zero padding in the evaluation of the autocorrelation function (ACF) showing uniform image data and the corresponding ACF in one dimension.

It is possible to evaluate the ACF via Fourier transforms since, according to the Wiener-Khinchin theorem, the ACF and the energy spectrum form a Fourier transform pair,

$$\phi_{11}(x,y) \Leftrightarrow F_1(u,v)\cdot F_1^*(u,v) = |F_1(u,v)|^2 \qquad (10)$$

where

$$f_1(x,y) \Leftrightarrow F_1(u,v)$$

It is possible to compute the ACF via the discrete Fourier transform using fast Fourier transform (FFT) techniques for computational speed, but this is not the most efficient technique for deriving the SNR. In the present application of the ACF, only the values of $\phi_{11}(x,y)$ in the vicinity of the origin, such as $\phi_{11}(1,0)$ and $\phi_{11}(0,1)$, are required to estimate $\phi_{11}^{NF}(0,0)$, and a direct computation of Eq. (9) will, in most cases, require fewer multiplications—only N^2 multiplications are needed per point. While evaluating the ACF via the Fourier transform returns the entire two-dimensional ACF, we are only interested in a few values at and around the origin.

In the computation of the ACF, one needs to consider the end effects. The practice to pad the ends of the array with zero is not appropriate in the present application, as this will exclude the contribution of the nonoverlapping ends to the value of the ACF. For example, consider an image of uniform intensity. If the image is zero padded, then the ACF will show a linear decrease from the origin (Fig. 8), where one would have expected a uniform ACF assuming that the image is part of a bigger picture of a similar intensity. Instead, it is suggested that the ends are padded with either the average value of the image, or the image is wrapped around, but only the N^2 values contained within the original image boundary are counted so as to preserve the total energy content of the image.

Intensity Saturation

In addition to the assumptions made under "Estimation of Noise-Free Autocorrelation" regarding the nature of the signal and noise components in SEM images, the issue of intensity saturation should also be considered. The SEM images are normally digitized as gray images with 256 intensity levels, with 0 representing absolute black and 255 absolute white. Quite often, SEM images contain pixels at either extreme of the intensity histogram, that is, they are saturated, based on typical brightness and contrast settings to produce pleasant-looking images that have the appearance of "good" contrast. Nevertheless, the portion of the histogram that represents saturated pixels is normally quite small unless the user chooses to exaggerate the contrast in the image.

The presence of noise broadens the histogram of the noise-free image. With high noise levels, the effect of intensity saturation changes the SNR of the image. If the histogram of the noise-free image is biased toward the black level, then the addition of noise of nominally zero mean will result in more pixels saturating at intensity level 0. Conversely, if the histogram is biased toward the white level, noise will cause more pixels to saturate at 255.

Figure 9 illustrates the effect of changing the brightness of a noisy image on the ACF. The brightness and contrast of the original noise-free image were adjusted to give a stretched histogram without much saturation. Noise was then added to this image (Fig. 9a), and the brightness adjusted by 10 (Fig. 9b) and 100 (Fig. 9c) intensity levels. By increasing the brightness values by 10, the ACF curve translates upward, but this does not affect the SNR significantly as the mean of the image also increases correspondingly provided that saturation does not occur. However, when a significant portion of the pixels is saturated (Fig. 9c), the signal level decreases for both noise-free and noisy images. As shown in Table II, for the noise-free image, the signal drops marginally from 150 to 149 because of a loss of image contrast with saturation, while the drop in the signal level for the noisy image is far greater to 112.3. The reason for this is that μ_1^2 for the noisy image is now considerably lower than that for the noise-free image, as the noise contribution to pixels at or near saturation is on the whole negative since positive noise excursions can at most saturate a pixel at 255. The same argument applies

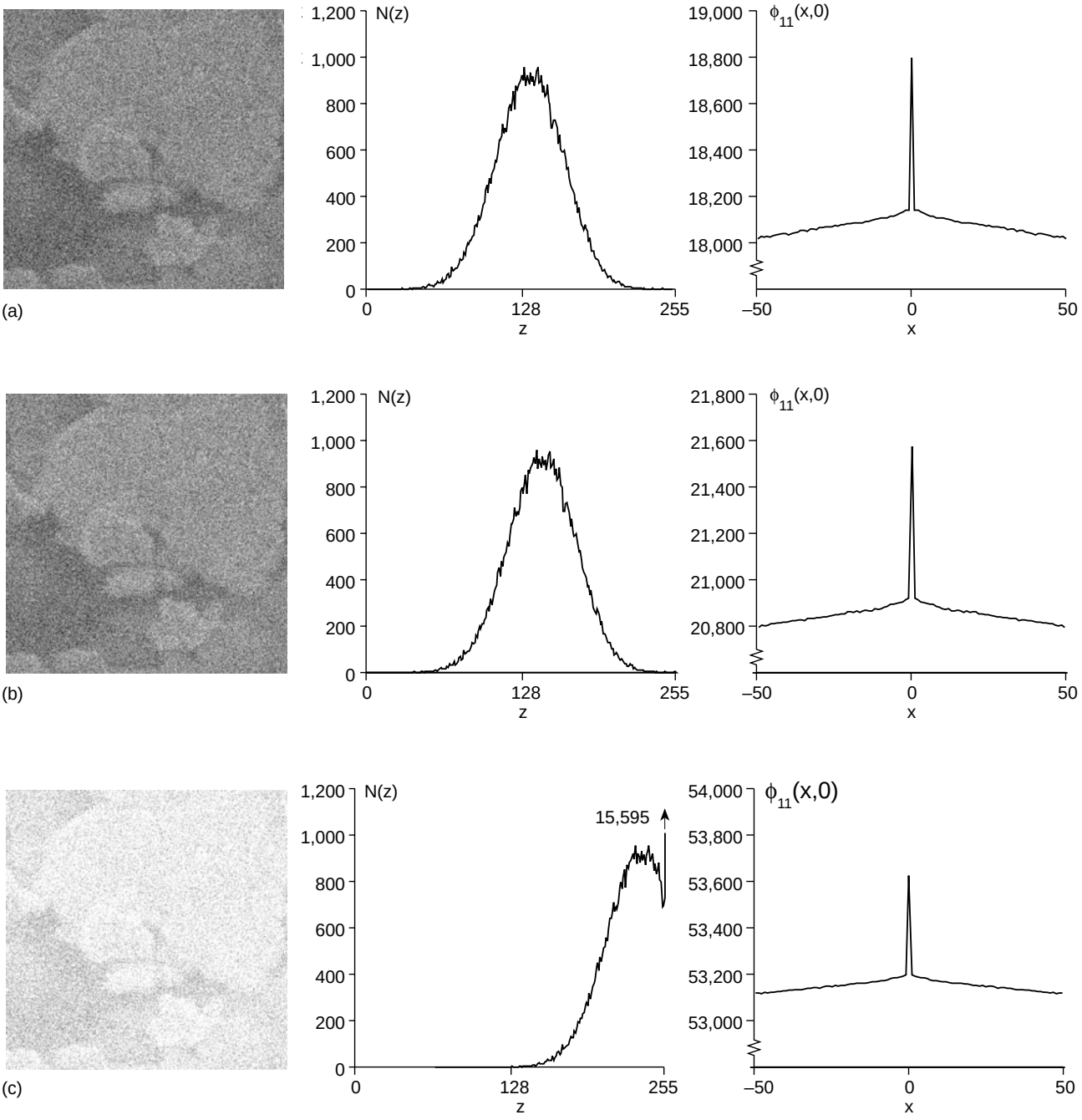

FIG. 9 Effect of image saturation on autocorrelation function (ACF). Image of silver paint with added noise (horizontal field width = 5 μm), intensity histogram, and ACF for (a) original image, (b) image with brightness increased by 10, and (c) image with brightness increased by 100 showing marked saturation at the white level.

TABLE II Parameters of original noise-free image and image with noise added at different brightness levels

	Noise-free image			Image + noise					
Image	μ_1^2	$\phi_{11}^{NF}(0)$	Signal	μ_1^2	$\phi_{11}(0)$	$\langle\phi_{11}^{NF}(0)\rangle$	Signal	Noise	SNR
$f_1(x,y)$	17992	18142	150	17991	18788	18136.0	145.0	652.0	0.222
$f_1(x,y) + 10$	20775	20925	150	20770	21574	20918.1	148.1	655.9	0.226
$f_1(x,y) + 100$	54805	54954	149	53102	53635	53214.3	112.3	420.7	0.267

Abbreviation as in Table I.

to the noise level which has dropped from 652.0 for the starting image to 420.7 for the brightest image. However, the compression of the noise is greater than the signal compression, and this results in the apparent improvement in SNR.

Conclusions

A method for estimating the SNR of a single image based on the autocorrelation function was developed. The requirements are that the noise should be white and that details in the image should correlate over distances of at least a few pixels, effectively separating the noise from signal. The ability to determine the SNR from a single image allows the technique to be applied to offline image analysis as well as to online applications, where the requirement of image registration with the traditional two-image technique is avoided. As the single-image technique needs only moderate amounts of computation, it can be applied to real-time SNR evaluation of SEM images and incorporated into the image averaging function to provide adaptive averaging where SNR is the parameter.

References

Erasmus SJ: Reduction of noise in TV rate electron microscope images by digital filtering. *J Microsc* 127 (Pt 1), 29–37 (1982)

Frank J: The role of correlation techniques in computer image processing. In *Computer Processing of Electron Microscope Images* (Ed. Hawkes PW). Springer-Verlag, Berlin 214–215 (1980)

Frank J: *Three-Dimensional Electron Microscopy of Macromolecular Assemblies*. Academic Press, San Diego, (1996) 109–110

Frank J, Al-Ali L: Signal-to-noise ratio of electron micrographs obtained by cross correlation. *Nature* 256, 376–379 (1975)

Joy DC, Ko YU, Hwu JJ: Metrics of resolution and performance for CD-SEMs in metrology inspection and process control for microlithography XIV. *Proc SPIE* 3998, 108–115 (2000)

Sijbers J, Scheunders P, Bonnet N, Van Dyck D, Raman E: Quantification and improvement of signal-to-noise ratio in a magnetic resonance image acquisition procedure. *Magnet Res Imag* 14, 1157–1163 (1996)